

## Surface Wettability-Enhanced Electrochemical Detection of Hydrogen Peroxide

Xiaoxia Su, Xiaomei Dong, Huile Jin<sup>\*</sup>, Tianqi Zhu, Chengzhan Yan, Aili Liu, Shun Wang<sup>\*</sup>

College of Chemistry and Materials Engineering, Wenzhou University, Wenzhou 325035, P. R. China

<sup>\*</sup>E-mail: [huilejin@wzu.edu.cn](mailto:huilejin@wzu.edu.cn); [shunwang@wzu.edu.cn](mailto:shunwang@wzu.edu.cn);

*Received:* 8 February 2017 / *Accepted:* 13 March 2017 / *Published:* 12 April 2017

---

A sensitive electrochemical sensor for the detection of hydrogen peroxide was fabricated in this study through manifesting surface wettability and morphology. Electrochemical measurements illustrate that a hydrophilic surface led to stronger electrocatalytic response of Pt to H<sub>2</sub>O<sub>2</sub>, yielding a sensitivity of 122.6  $\mu\text{A}\cdot\text{mM}^{-1}\cdot\text{cm}^{-2}$  within the concentration range between 40 and 500 nM. The achieved low detection limit is 12.8 nM. The hydrophilic surface also exhibits positive influences on the selectivity of H<sub>2</sub>O<sub>2</sub> over ascorbic acid and ethanol. The observation highlights the importance of macroscopic properties such as surface wettability in the development of sensitive and selective chemical sensors.

---

**Keywords:** Surface wettability, Electrochemical catalysis, Hydrogen peroxide, Pt nanoparticle.

### 1. INTRODUCTION

The detection of hydrogen peroxide is an important task in many areas including food industry, pharmaceutical and environmental analyses[1-2]. Several analytical methods on the basis of fluorescence, chemiluminescence or electrochemical processes have been developed for the detection of H<sub>2</sub>O<sub>2</sub>[3-8]. Electrochemical detection of H<sub>2</sub>O<sub>2</sub> has attracted a great deal of attention for its low detection limit as well as low costs[9-11], where biomolecules such as peroxidase enzymes and proteins have been used to modify the electrode in order to achieve a great selectivity and sensitivity[12-13]. Such a procedure unfortunately leads to limited lifetime and stability problem of the sensor, needless to say that the preparation of the sensor was also complicated by the involvement of biomolecules. To overcome the above shortcoming encountered in the electro-biochemical detection, enzyme-free H<sub>2</sub>O<sub>2</sub> sensors have been actively pursued through using noble metals nanoparticles, metal oxides or conductive polymers to construct the working electrode[14-22]. For example, Pt nanoparticles have been employed as an anode, showing excellent performance in catalyzing the

reaction process of  $\text{H}_2\text{O}_2$ [23-29]. However, further improving the selectivity and sensitivity of the enzyme-free Pt-based sensors remains to be a challenge.

Nanomaterials provide a large number of active sites for surface reactions, however their chemical and physical properties are greatly affected by the size and morphology. It has been reported that the assembly of different sized nanoparticles may result in very different surface wettability[30-32]. While the importance of surface wettability has been well recognized in heterogeneous chemical reactions, it has been largely ignored in the fabrication of electrochemical sensors. To shed light on this subject, in the present work we used an electrochemical approach to generate Pt nanoparticles on a clean indium tin oxide (ITO) glass substrate. The electrochemical deposition method is of simple operation, environmentally benign and easy to control, readily producing Pt films with a wide range of surface wettability (i.e., from hydrophobic to nearly superhydrophobic). The method complements the reported synthesis of Pt nanoparticles, which often involved complicated preparation processes and costly materials[33-36]. Electrochemical measurements illustrate that surface wettability has significant effect on the selectivity and sensitivity in detecting  $\text{H}_2\text{O}_2$ . Using chronoamperometry method the low detection limit of  $\text{H}_2\text{O}_2$  in a phosphate buffer solution was found to be around 12.8 nM (S/N = 3), which is significantly better than those achieved with a regular Pt electrode.

## 2. EXPERIMENTAL

### 2.1. Materials and apparatus

$\text{H}_2\text{O}_2$  (30%),  $\text{H}_2\text{PtCl}_6$ , and  $\text{H}_2\text{SO}_4$  (95-98%) were purchased from Alfa Aesar. Indium tin oxide (ITO) ( $1.0 \times 2.0 \text{ cm}^2$ ) glass was purchased from Laibao Electrical Company (Shenzhen, China). Fresh  $\text{H}_2\text{O}_2$  solution was prepared daily. Phosphate buffer solution (PBS, 0.1 M pH 7.0) was prepared by mixing standard solutions of  $\text{Na}_2\text{HPO}_4$  and  $\text{NaH}_2\text{PO}_4$ . Deionized water was prepared with a Milli-Q system (Millipore, USA). Scanning electron microscopy (SEM) was carried out with a Nova NanoSEM 200 (FEI, Inc.). Transmission electron microscopy (TEM) was performed with a Hitachi model H-800 transmission electron microscope. Electrochemical measurements were performed at room temperature with a CHI660C electrochemical workstation (Shanghai Chenhua Instrumental Co., Ltd., China), where the counter and the reference electrodes were platinum wire and a saturated Ag/AgCl electrode, respectively. The Pt coated ITO electrodes were used as the working electrode. Before the measurements, the solution was deaerated with pure nitrogen gas for 3 minutes.

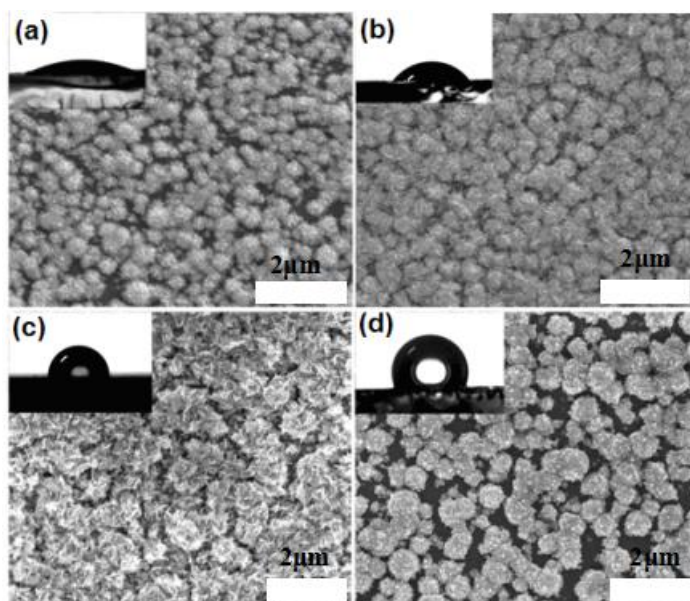
### 2.2. Preparation of Pt electrodes

Before the electrodeposition, the ITO substrate was ultrasonicated sequentially in acetone, ethanol and deionized water for 15 min each. The electrochemical reduction was conducted in a solution containing 0.18 mM  $\text{H}_2\text{PtCl}_6$  and 0.25 M  $\text{H}_2\text{SO}_4$  at an applied potential of  $-0.2 \text{ V}$  vs Ag/AgCl electrode. By controlling the deposition time a series of Pt films were obtained. The surface wettability

of those Pt films was measured with a SL200B instrument (Solon Tech, Shanghai, China), where the water contact angle was measured at four different spots of each surface and an average value was reported. The effective surface areas (ESA) of the Pt layer was determined using the method and parameters reported in literature[37].

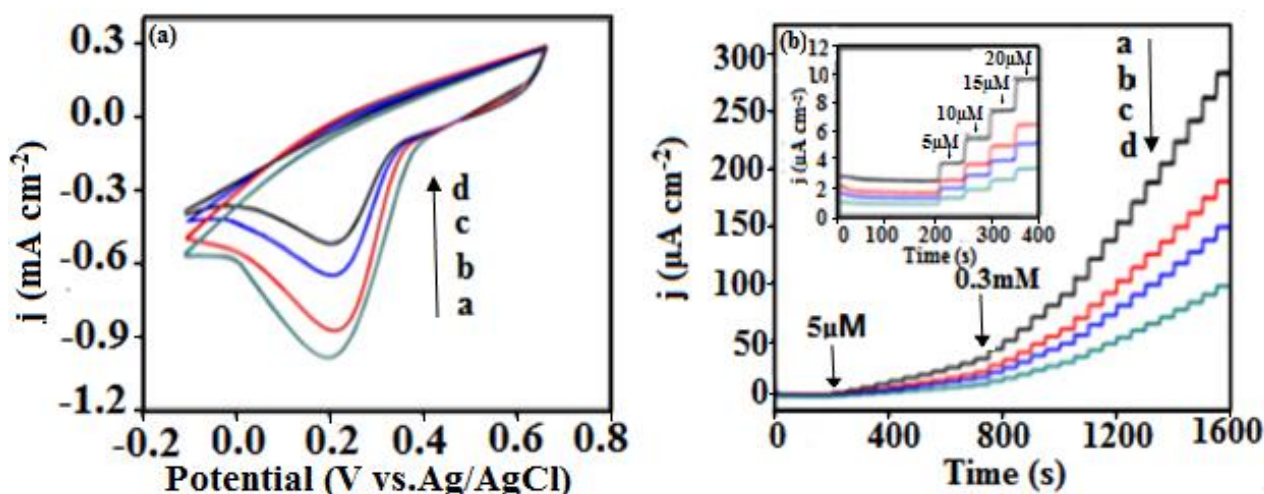
### 3. RESULTS AND DISCUSSION

Fig. 1 presents the SEM images of 4 Pt films prepared with a deposition time of (a) 100 s, (b) 400 s, (c) 600 s and (d) 800 s. These images illustrate that the Pt films are made up by many nanoparticles and the morphology of those nanoparticles are different at different deposition times. The ITO substrate appears to be only partially covered by Pt deposits, however carefully examination indicates that the ITO glass is fully covered by Pt products for a deposition time less than 100 s. The inset in Fig. 1a illustrates that this Pt film has a water contact angle of  $24.0 \pm 1.2^\circ$  (i.e., it is a hydrophilic surface). As the deposition time was increased to 400 s, these nanoparticles grew into different shapes, resulting in an increase of the water contact angle to  $51.0 \pm 0.9^\circ$ . In other words, the wettability of the surface has decreased as a result of prolonging the reaction time. Further increasing the electrochemical reduction time to 600 s, the surface of those nanoparticles in Fig. 1c became rougher, leading to further increase of the contact angle to  $80.0 \pm 0.5^\circ$ . When the Pt deposition time was increased to 800 s in Fig. 1d, the inset shows that the average contact angle of the Pt layer has increased to  $104.0 \pm 0.4^\circ$ , turning into a hydrophobic surface as a result of merely varying the deposition time.



**Figure 1.** SEM images of the Pt films prepared with a deposition time of (a) 100 s, (b) 400 s, (c) 600 s and (d) 800 s. The electrolyte consists of 0.18 mM  $\text{H}_2\text{PtCl}_6$  and 0.25 M  $\text{H}_2\text{SO}_4$  electrolyte. The insets show the measured contact angles: (a)  $24.0 \pm 1.2^\circ$ , (b)  $51.0 \pm 0.9^\circ$ , (c)  $80.0 \pm 0.5^\circ$ , and (d)  $104.0 \pm 0.4^\circ$ .

Electrochemical performance of the above 4 Pt electrodes was tested in a PBS solution containing 0.08 mM  $\text{H}_2\text{O}_2$ . As shown in Fig. 2(a), different behaviors are observed at the four Pt electrodes. Due to the sluggish oxidation of  $\text{H}_2\text{O}_2$  at Pt electrode, the anodic peak is not obvious on the forward scan. However, the cathodic peaks on the reverse scan could be identified easily. Importantly, as the wettability of Pt film decreased, the peak current also decreased accordingly, where the Pt electrode having the largest water contact angle yielded the lowest peak. To further confirm the above observation that the surface wettability may play a rather important role in the electrochemical detection of  $\text{H}_2\text{O}_2$ , amperometric responses of the above four Pt electrodes to the addition of  $\text{H}_2\text{O}_2$  were tested in Fig. 2(b). These experiments were conducted under constant stirring at an applied potential of 0.32 V. Results in Fig. 2(b) show that all four Pt@ITO electrodes responded quickly to the change of  $\text{H}_2\text{O}_2$  concentration, reaching a steady-state signal within 2 s. The response current decreased with respect to the surface wettability and the largest response was achieved with the Pt electrode having the strongest hydrophilic surface.



**Figure 2.** (a) CVs of Pt electrodes in  $\text{H}_2\text{O}_2$  solution, (b) amperometric responses of the Pt electrodes to the successive injection of  $\text{H}_2\text{O}_2$  into a PBS solution. Surface wettability of the four Pt electrodes used is (a)  $24.0 \pm 1.2^\circ$ , (b)  $51.0 \pm 0.9^\circ$ , (c)  $80.0 \pm 0.5^\circ$ , and (d)  $104.0 \pm 0.4^\circ$ . The scan rate in (a) was  $50 \text{ mVs}^{-1}$  and the applied potential was 0.32 in (b).

The above experiments clearly demonstrate that tuning the surface wettability can improve Pt performance. Along this direction, a new Pt electrode with even higher surface wettability was fabricated by using different deposition conditions (0.10 mM  $\text{H}_2\text{PtCl}_6 + 0.25 \text{ M H}_2\text{SO}_4$  electrolyte for a deposition of 300 s at an applied potential of -0.2 V). SEM image in Fig. 3a shows the morphology of the Pt film, where a large number of nanoparticles with a size of around 50 nm are scattered evenly on the surface. Different from the microstructures seen in Fig. 1a, here the surface of these nanoparticles appears to be smooth, which is likely responsible for the increase of the surface wettability (see the inset for the measurement of the water contact angle  $14.0 \pm 1.3^\circ$ ). The EDX measurements in Fig. 3d indicate that those Pt particles are pure, in which the copper and carbon peaks in the spectrum arise from the substrate used to prepare the specimen. According to the HRTEM in Fig. 3b, these pure Pt

crystals preferably grew along {111} direction. The selected area electron diffraction analysis in Fig. 3c demonstrates that these Pt nanoparticles are polycrystalline.

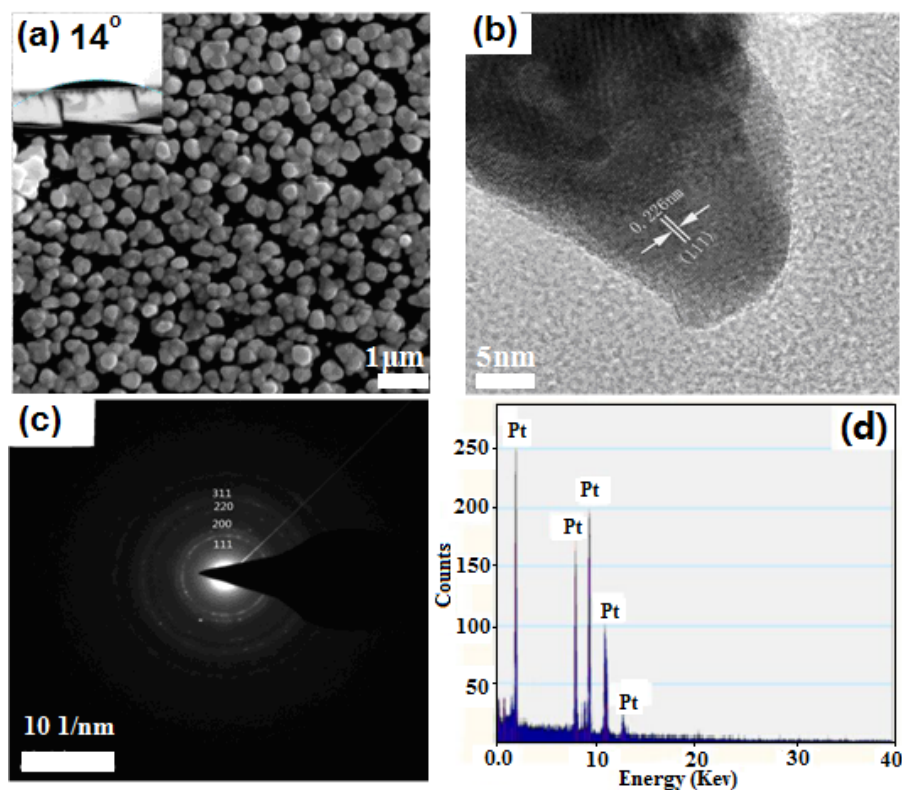


**Figure 3.** (a) SEM image, (b) HRTEM image, (c) selected area electron diffraction (SAED), (d) EDX of Pt deposit on an ITO substrate, Here the deposition tool place in 0.10 mM  $\text{H}_2\text{PtCl}_6$  + 0.25 M  $\text{H}_2\text{SO}_4$  electrolyte for 300 s at an applied potential of - 0.2 V. The inset in (a) is the measurement of the surface wettability.

Amperometric response of the above hydrophilic Pt electrode to the addition of  $\text{H}_2\text{O}_2$  was characterized in Fig. 4(a), which shows that the Pt@ITO electrode responds quickly to the change of  $\text{H}_2\text{O}_2$  concentration, reaching a steady-state signal within 2 s. The corresponding calibration curve is shown in Fig. 4(b), which indicates that the Pt sensor has two linear response windows with respect to  $\text{H}_2\text{O}_2$  concentration and appears to be more sensitive within the low  $\text{H}_2\text{O}_2$  concentration range. The sensitivities (i.e., slopes of the calibration line) within the low concentration range is  $122.6 \mu\text{A mM}^{-1} \text{cm}^{-2}$  with a linear correlation coefficient of 0.998. For this hydrophilic Pt sensor, the low detection limit is calculated to be 12.8 nM using  $S/N = 3$ , which is significantly better than that achieved with earlier Pt-based nonenzymatic  $\text{H}_2\text{O}_2$  sensors[24-30].

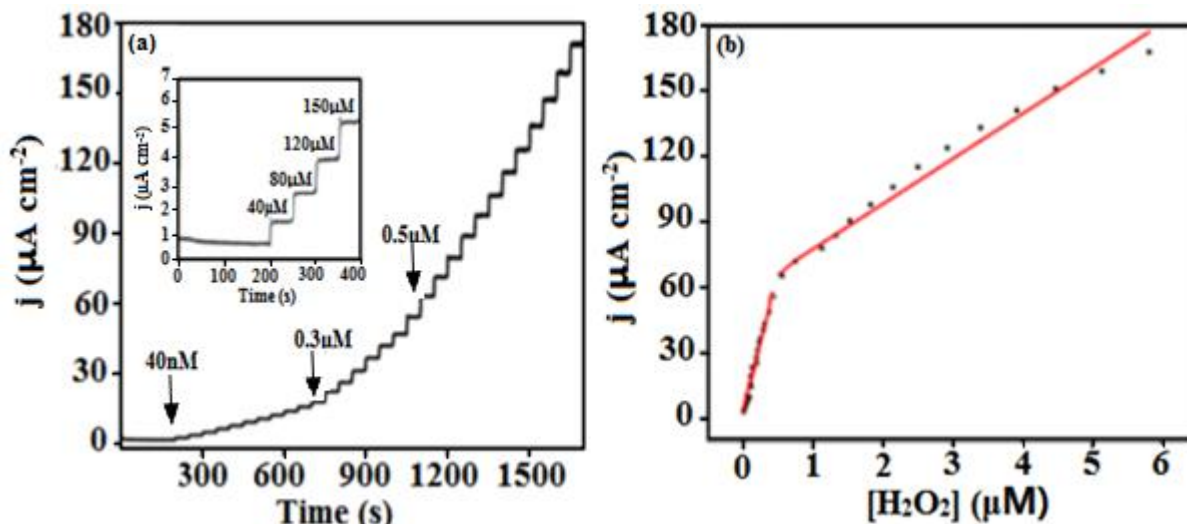


**Figure 4.** (a) amperometric responses of the Pt electrode to the successive injection of H<sub>2</sub>O<sub>2</sub> into a PBS solution, and (b) a calibration curve of the response current versus H<sub>2</sub>O<sub>2</sub> concentration. The water contact angle of this Pt electrode is 14.0±1.3°.

The selectivity of the above Pt sensor was evaluated with ascorbic acid (AA) and ethanol. When 0.01 mM of H<sub>2</sub>O<sub>2</sub>, 0.1 mM AA or CH<sub>3</sub>CH<sub>2</sub>OH was injected into the PBS solution, significantly different response currents were observed as shown in Fig. 5. This suggests that these species have no obvious interference on the electro-oxidation of H<sub>2</sub>O<sub>2</sub>.

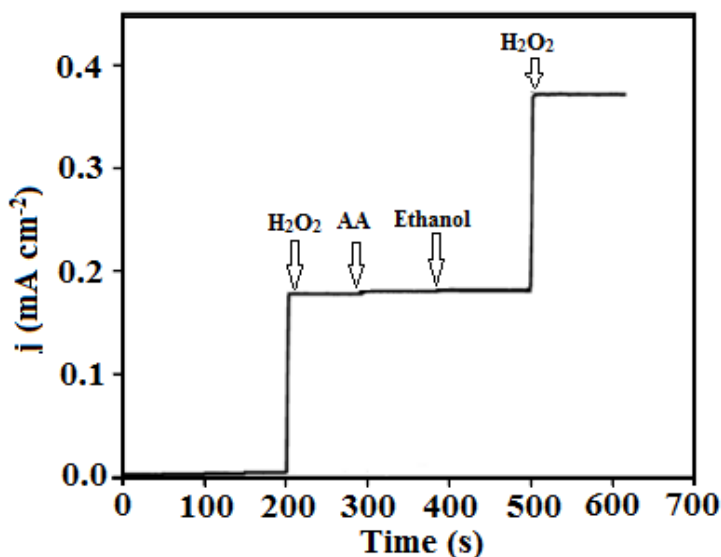


**Figure 5.** Response currents to the addition of 0.01 mM H<sub>2</sub>O<sub>2</sub>, 0.1 mM AA, or 0.1 mM ethanol. The water contact angle of this Pt electrode is 14.0±1.3°, and the applied potential is 0.32 V.

The comparing with several previous reports reported in the literature and shown in Table 1 in terms of applied potential, linear range, sensitivity and detection limit. As can be seen, the fabricated H<sub>2</sub>O<sub>2</sub> sensor herein had comparative or even better advantages in lower detection limit than reported of

PDDA/t-GO-Pt/GCE (0.65  $\mu\text{M}$ ) [24], Pt (0.20  $\mu\text{M}$ ) [25], Pt-SnO<sub>2</sub>@C (0.10  $\mu\text{M}$ ) [26], Pt (0.010  $\mu\text{M}$ ) [32], Pt-Cu@PSi-CILE (0.10  $\mu\text{M}$ ) [39], Pt@Au/EDA (0.18  $\mu\text{M}$ ) [42] et al., which is an attractive feature for the determination of H<sub>2</sub>O<sub>2</sub> at low concentrations. These could be attributed to the stronger hydrophilic surface property. Therefore, it is clear that the proposed hydrophilic surface Pt sensor exhibits a better performance than many other H<sub>2</sub>O<sub>2</sub> sensor .

**Table 1.** Performance of various nonenzymatic H<sub>2</sub>O<sub>2</sub> electrochemical sensors.

Catalyst composition	Detection potential (V)	Linear range ( $\mu\text{M}$ )	Sensitivity ( $\mu\text{A}\cdot\text{mM}^{-1}\cdot\text{cm}^{-2}$ )	Detection limit ( $\mu\text{M}$ )	References
PDDA/t-GO-Pt/GCE	-0.1(Ag/AgCl)	0.001-5	353.86	0.65	[24]
PDDA/t-MWCNT-Pt/GCE	-0.1(Ag/AgCl)	0.001-8	481.25	0.27	[24]
Pt	-0.08(Ag/AgCl)	0.5-3475	459.00 $\pm$ 3	0.20	[25]
Pt-SnO <sub>2</sub> @C	0.5(Ag/AgCl)	1-170	241.10	0.10	[26]
GN-Pt	-0.2(Ag/AgCl)	2-710	-	0.50	[27]
Pd <sub>70</sub> Pt <sub>30</sub>	0.0(Ag/AgCl)	0-500	102.00	-	[28]
Se/Pt	0.0 (SCE)	10-15000	-	3.10	[29]
Pt-Pd	-0.4(Ag/AgCl)	5-6000	804.00	0.87	[30]
NiHCF/GS/Pt/n-n+-Si	0.0(SCE)	2-2900	3530	1.00	[31]
Pt	-0.05(Ag/AgCl)	0.1-25	1410	0.01	[32]
Pt /porous graphene	-0.1(Ag/AgCl)	1-1477	341.14	0.50	[33]
Pt@UiO-66	0.85(Hg/HgO)	5-14750	75.33	3.06	[34]
RGO/CS/Fc/Pt	-0.05(SCE)	0.02-3 6-10000	-	0.02	[35]
Pt-CNFs	-0.1 (Ag/AgCl)	10-1000	147.8	0.000195	[36]
Fe@Pt/C	-0.55(SCE)	2.5-41605	218.97	0.75	[37]
Pd core-Pt NDs-rGO	0.018(Ag/AgCl)	5-500	627.753	0.027	[38]
Pt-Cu@PSi-CILE	-0.25(Ag/AgCl)	0.5-1280	-	0.10	[39]
Pt-MnO <sub>x</sub> @C	0.35(Ag/AgCl)	2-4000	122.99	0.70	[40]
Au@C@Pt	0.0(Ag/AgCl)	9-1860 1860-7110	144.7 80.1	0.136	[41]
Pt@Au/EDA	0.08(Ag/AgCl)	1-450	-	0.18	[42]
Pt/CNF	0.0(Ag/AgCl)	1-800	-	0.6	[43]
PtNps/GCNF	0.3(Ag/AgCl)	10-2000	41.3 $\pm$ 0.546	6.9	[44]
Pt films	-0.2(Ag/AgCl)	0.04-0.5	122.6	0.0128	This work

#### 4. CONCLUSION

Using a simple electrochemical method, nonenzymatic H<sub>2</sub>O<sub>2</sub> sensors consisting of Pt nanoparticles were fabricated. Comparing with existing Pt-based H<sub>2</sub>O<sub>2</sub> sensors, this new platform exhibits greatly improved sensitivity and a low detection limit. Equally significant, this study demonstrates that Pt nanoparticles with a stronger hydrophilic surface property have a larger electrocatalytic response to H<sub>2</sub>O<sub>2</sub>, offering a new direction to further improve the sensitivity of electrochemical sensors. Because of the simplicity of the preparation method, the as-prepared Pt electrodes are expected to find important applications in different fields such as electrode materials, fuel cells, and catalysts.

#### ACKNOWLEDGMENTS

We are grateful for financial supports from National Natural Science Foundation of China (21471116, 21628102, 21601138, 21475097 and 21301130), Zhejiang Provincial Natural Science Foundation of China (LZ15E020002, Y17E020012 and LZ17E020002) and Xinmiao Talents Program of Zhejiang province (2016R426025).

#### References

1. W. Chen, S. Cai, Q. Q. Ren, W. Wen, Y. D. Zhao, *Analyst*, 137 (2012) 49-58.
2. D. Chirizzi, M. R. Guascito, E. Filippo, C. Malitesta, A. Tepore, *Talanta*, 147 (2016) 124-131.
3. M. Q. Wang, Y. Zhang, S. J. Bao, *Electrochim. Acta*, 190 (2016) 365-370.
4. Z. Y. Li, J. Li, L. P. Du, M. Y. Li, Y. M. Shen, *Sci China Chem*, 42 (2012) 1683-1693.
5. J. L. Liu, L. L. Lu, A. Q. Li, J. Tang, S. G. Wang, S. Y. Xu, L. Y. Wang, *Biosens. Bioelectron.*, 68 (2015) 204-209.
6. W. Sun, Z. Ma, J. Li, W. H. Li, L. P. DU, M. Y. Li, *Sci China Chem*, 56 (2013) 1440-1445.
7. H. M. Li, L. Li, X. Wang, Q. L. Li, M. Du, B. Tang, *Sci China Chem*, 58 (2015) 825-829.
8. J. J. Zhang, Y. G. Liu, L. P. Jiang, J. J. Zhu, *Electrochem. Commun.*, 10 (2008) 355-358.
9. X. L. Sun, S. J. Guo, C. S. Chung, W. L. Zhu, S. H. Sun, *Adv. Mater.*, 25 (2013) 132-136.
10. K. C. Fang, C. P. Hsu, Y. W. Kang, J. Y. Fang, C. C. Huang, C. H. Hsu, Y. F. Huang, C. C. Chen, S. S. Li, J. A. Yeh, D. J. Yao, Y. L. Wang, *Biosens. Bioelectron.*, 55 (2014) 294-300.
11. H. Mei, W. Q. Wu, H. M. Wu, S. F. Wang, Q. H. Xia, *Sensor. Actuat. B-chem.*, 223 (2016) 68-75.
12. D. R. Jin, K. Sakthivel, S. Gandhi, B. T. Huy, Y. L. Lee, *Sensor. Actuat. B-chem.*, 237 (2016) 81-89.
13. S. Komathi, A. I. Gopalan, S. K. Kim, G. S. Anand, K. P. Lee, *Electrochim. Acta*, 92 (2013) 71-78.
14. J. K. Lee, J. Choi, S. J. Kang, J. M. Lee, Y. Tak, J. Lee, *Electrochim. Acta*, 52 (2007) 2272-2276.
15. G. Q. Sun, L. N. Zhang, Y. Zhang, H. M. Yang, C. Ma, S. G. Ge, M. Yan, J. H. Yu, X. R. Song, *Biosens. Bioelectron.*, 71 (2015) 30-36.
16. S. Palanisamy, S. M. Chen, R. Sarawathi, *Sensor. Actuat. B-chem.*, 166-167 (2012) 372-377.
17. Y. Zhang, C. Y. Wu, X. J. Zhou, X. C. Wu, Y. Q. Yang, H. X. Wu, S. E. Guo, J. Y. Zhang, *Nanoscale*, 5 (2013) 1816-1819.
18. P. Bhatia, P. Yadav, B. D. Gupta, *Sensor. Actuat. B-chem.*, 182 (2013) 330-335.
19. J. Ju, W. Chen, *Anal. Chem.*, 87 (2015) 1903-1910.
20. C. Yang, L. W. Hu, H. Y. Zhu, Y. Ling, J. H. Tao, C. X. Xu, *J. Mater. Chem. B*, 3 (2015) 2651-2659.

21. J. Bai, X. E. Jiang, *Anal. Chem.*, 85 (2013) 8095–8101.
22. H. F. Chen, X. P. Wang, G. T. Liu, A. J. Lin, Y. Wen, H. F. Yang, *Sci China Chem*, 58 (2015) 1-7.
23. J. You, M. D. Kim, *Electrochim Acta*, 65 (2012) 288–293.
24. Y. Y. Zhang, X. Y. Bai, X. M. Wang, K. K. Shiu, Y. L. Zhu, H. Jiang, *Anal. Chem.*, 86 (2014) 9459–9465.
25. H. T. Lu, Yu, Y. Fan, C. P. Yang, D. L. Xu, *Colloids Surf., B.*, 101 (2013) 106–110.
26. F. Xu, Y. J. Sun, Y. Zhang, Y. Shi, Z. W. Wen, Z. Li, *Electrochem. Commun.*, 13 (2011) 1131-1134.
27. F. C. Nagaiah, D. D. Schafer, W. W. Schuhmann, N. Dimcheva, *Anal. Chem.*, 85 (2013) 7897–7903.
28. Y. Li, J. J. Zhang, J. Xuan, L. Jiang, J. Zhu, *Electrochem. Commun.*, 12 (2010) 777-780.
29. X. H. Niu, C. Chen, H. L. Zhao, Y. Chai, M. B. Lan, *Biosens. Bioelectron.*, 36 (2012) 262–266.
30. K. N. Han, C. A. Li, M. P. N. Bui, X. H. Pham, B. S. Kim, Y. H. Choa, G. H. Seong, *Sensor. Actuat. B-chem.*, 174 (2012) 406-413.
31. H. Zhang, Q. Gao, H. X. Li, *J. Solid State Electr.*, 20 (2016) 1565–1573.
32. Y. Sun, K. He, A. Zhou, H. Duan, *Biosens. Bioelectron.*, 68 (2015) 358–364.
33. J. Liu, X. J. Bo, Z. Zheng, L. P. Guo, *Biosens. Bioelectron.*, 74 (2015) 71-77.
34. Z. D. Xu, L. Z. Yang, C. L. Xu, *Anal. Chem.*, 87 (2015) 3438-3444.
35. Z. H. Bai, G. Y. Li, K. Hnida, J. T. Liang, J. Su, Y. Zhang, H. Z. Chen, Y. Huang, W. G. Sui, Y. X. Zhao, *Biosens. Bioelectron.*, 82 (2016) 185-194.
36. T. Laurila, S. Sainio, H. Jiang, N. Isoaho, J. E. Koehne, J. Etula, J. Koskinen, M. Meyyappan, *ACS Omega*, 2 (2017) 496-507.
37. H. Mei, B. B. Yu, H. M. Wu, S. F. Wang, Q. H. Xia, *Sensor. Actuat. B-chem.*, 223 (2016) 68-75.
38. Y. Y. Zhang, C. Zhang, D. Zhang, M. Ma, W. Z. Wang, Q. Chen, *Mat. Sci. Eng. C.*, 58 (2016) 1246-1254.
39. A. A. Ensafi, M. M. Abarghoui, B. Eezaei, *Electrochim. Acta*, 190 (2016) 199-207.
40. H. L. Kivrak, O. Alal, D. Atbas, *Electrochim. Acta*, 176 (2015) 497-503.
41. Y. Y. Zhang, Y. H. Li, Y. Y. Jiang, Y. C. Li, S. X. Li, *Appl. Surf. Sci.*, 378 (2015) 375-383.
42. Y. Li, Q. Lu, S. Wu, L. Wang, X. Shi, *Biosens. Bioelectron.*, 41 (2013) 576–581.
43. Y. Liu, D. Wang, L. Xu, H. Hou, T. You, *Biosens. Bioelectron.*, 26 (2011) 4585–4590.
44. O. A. Loaiza, P. J. L. Ardisana, L. Anorga, E. Jubete, V. Ruiz, M. Borghei, H. J. Grande, *Bioelectrochemistry*, 101 (2015) 51-65.